CHINESE JOURNAL OF PHYSICS VOL. 52, NO. 1-II February 2014

Review

Quantum Orbits: a Powerful Concept in Laser-Atom Physics*

Wei Quan,[1] XuanYang Lai,[1] YongJu Chen,[1,2] ChuanLiang Wang,[1,2] ZiLong Hu,[1,2] XiaoJun Liu,[1,†] XiaoLei Hao and Jing Chen,[3,4,‡] Elvedin Hasović,[5] Mustafa Busuladžić,[6] Dejan B. Milošević,[5,7,8,§] and Wilhelm Becker[8,¶]

[1]*State Key Laboratory of Magnetic Resonance and Atomic and Molecular Physics, Wuhan Institute of Physics and Mathematics, Chinese Academy of Sciences, Wuhan 430071, China*
[2]*University of Chinese Academy of Sciences, Beijing 100080, China*
[3]*HEDPS, Center for Applied Physics and Technology, Peking University, Beijing 100084, China*
[4]*Institute of Applied Physics and Computational Mathematics, P. O. Box 8009, Beijing 100088, China*
[5]*Faculty of Science, University of Sarajevo, Zmaja od Bosne 35, 71000 Sarajevo, Bosnia and Herzegovina*
[6]*Medical Faculty, University of Sarajevo, Čekaluša 90, 71000 Sarajevo, Bosnia and Herzegovina*
[7]*Academy of Sciences and Arts of Bosnia and Herzegovina, Bistrik 7, 71000 Sarajevo, Bosnia and Herzegovina*
[8]*Max Born Institute for Nonlinear Optics and Short-Pulse Spectroscopy, Max-Born-Str. 2a, 12489 Berlin, Germany*

(Received October 3, 2013)

Additional support for the concept of "quantum orbits" is presented that emphasizes in particular the importance of "long orbits" where the time between ionization and rescattering may be many periods of the laser field. Two examples are discussed, above-threshold ionization by an elliptically polarized laser field and intensity-dependent enhancements of certain spectral regions within the backscattering plateau, where we compare experimental data and the theoretical quantum-orbit simulations. In both cases, good agreement is obtained.

DOI: 10.6122/CJP.52.389 PACS numbers: 33.80.Rv, 33.80.Wz, 42.50.Hz

I. INTRODUCTION

Atoms irradiated by intense laser fields that are strong enough to liberate one or several electrons have presented an enormous challenge to theory. The electron interacting

* This paper is dedicated to Professor See Leang Chin on the occasion of his official retirement.

†Electronic address: xjliu@wipm.ac.cn
‡Electronic address: chen_jing@iapcm.ac.cn
§Electronic address: milo@bih.net.ba
¶Electronic address: wbecker@mbi-berlin.de

with either the Coulomb field without the laser field or with the laser field without the Coulomb field allow for analytical solutions, but the combination of the two fields has resisted any straightforward analytical attack. Of course, with currently available computing power solution of the time-dependent one-electron Schrödinger equation has become standard. But if there is more than one electron then even today's computing facilities quickly reach their limits. Moreover, solutions of the TDSE call for an interpretation just like real experiments.

It is here where the theory of "quantum orbits" comes in. It derives from the strong-field approximation (SFA) [1, 2], which accounts for the Coulomb interaction only in the initial bound state of the electron, or from the improved SFA (ISFA), which includes exactly one additional interaction of the liberated electron with the binding potential [3, 4]. This is analogous to the first term of the Born series. The ISFA allows the analysis of rescattering processes, which are central to current strong-field physics and have, via the process of high-order harmonic generation (HHG), opened the door to attosecond science [5]. Here, we will restrict ourselves to above-threshold ionization (ATI), but HHG and other processes such as field-assisted electron-atom scattering or nonsequential double ionization can be and have been treated along the same lines [6].

Quantum orbits provide a good approximation under conditions where the electron can be envisioned as being liberated by the process of tunneling through the time-dependent barrier that is formed by the binding potential plus the electron-field interaction $\mathbf{r} \cdot \mathbf{E}(t)$. Actually, it does not matter exactly how the electron gets out of the atom, as long as it makes sense to assume that this happens at a fairly well-defined time and position. The quantum orbits then depict the electronic trajectory from this point, the "exit of the tunnel," toward the detector at infinity within the limitation pointed out above: at most one interaction with the potential. Otherwise, they are much like classical trajectories. However, they are complex in consequence of their origin via tunneling and they interfere if more than one orbit leads from the initial bound state to the final plane-wave state. The (I)SFA and quantum orbits allow one directly to calculate approximations to individual S-matrix elements, which are specified by the asymptotic momentum $\mathbf{p}$ of the electron in its final state. This is in contrast to solution of the TDSE, where first the wave function has to be computed in its entirety and to be stored, before such matrix elements can be evaluated.

Usually, there are many different quantum orbits that lead from the same initial into the same final state. They can be characterized by the length of their "travel time," that is, by the difference between the time when the electron has its final recollision with its parent ion and the time when it is liberated by tunneling. Formally, there are orbits with longer and longer travel times, limited only by the duration of the laser pulse. It is tempting to assign some physical reality to the quantum orbits and also to these "longer orbits." In this paper, we review two recent experiments and their quantum-orbit interpretations, which provide additional support for their physical significance.

In the next Section, we briefly review the concept and the formalism of quantum orbits. Thereafter, we focus on the two recent examples: ATI by an elliptically polarized laser field where the dominant contribution comes from orbits with travel times longer

than that of the shortest two orbits [7], and the intensity-dependent enhancements in ATI spectra of molecules [8]. The paper is terminated by our conclusions.

More detailed reviews of the theory and applications of quantum orbits can be found in Refs. [9–11]. We use atomic units such that $|e| = m = \hbar = 1$ throughout the paper.

II. QUANTUM ORBITS

Quantum-orbit theory starts from the strong-field approximation (SFA) for "direct" electrons, i.e. those that after they have been liberated from their parent ion do not interact with it any more, or from the "improved" strong-field approximation (ISFA), which allows for one such interaction. The latter corresponds to the first-order Born approximation for the liberated electron revisiting the ion. The ionization amplitude is the sum of the "direct" amplitude

$$M_{\mathbf{p}}^{(0)} = \int_{-\infty}^{\infty} dt' \langle \psi_{\mathbf{p}}^{V}(t') | \mathbf{r} \cdot \mathbf{E}(t') | \psi_0(t') \rangle \tag{1}$$

and the rescattering amplitude

$$M_{\mathbf{p}}^{(1)} = \int_{-\infty}^{\infty} dt \int_{-\infty}^{t} dt' \langle \psi_{\mathbf{p}}^{V}(t) | V U^{V}(t,t') \mathbf{r} \cdot \mathbf{E}(t') | \psi_0(t') \rangle. \tag{2}$$

The final state is a Volkov state

$$\langle \mathbf{r} | \psi_{\mathbf{p}}^{V}(t) \rangle = (2\pi)^{-\frac{3}{2}} e^{i[\mathbf{p}+\mathbf{A}(t)]\cdot\mathbf{r}} \times \exp\left(-\frac{i}{2} \int^{t} d\tau [\mathbf{p} + \mathbf{A}(\tau)]^2 \right) \tag{3}$$

with asymptotic (drift) momentum $\mathbf{p}$, and the ISFA amplitude (2) contains the corresponding Volkov time-evolution operator $U^{V}(t,t')$. While the times t' and t are, of course, just integration variables, we will see below that it is suggestive to interpret them as the times of ionization and recollision, respectively.

Henceforth, we will focus on the ISFA amplitude (2). It is convenient to expand the Volkov time-evolution operator in terms of the Volkov states (3),

$$U^{V}(t,t') = \int d^3\mathbf{k} |\psi_{\mathbf{k}}^{V}(t)\rangle \langle \psi_{\mathbf{k}}^{V}(t')|, \tag{4}$$

which is here given in length gauge. The ISFA amplitude then has the structure

$$M_{\mathbf{p}}^{(1)} = \int_{-\infty}^{\infty} dt \int_{-\infty}^{t} dt' \int d^3\mathbf{k} e^{iS_{\mathbf{p}}(t,t',\mathbf{k})} m_{\mathbf{p}}(t,t',\mathbf{k}) \tag{5}$$

where $m_{\mathbf{p}}(t,t',\mathbf{k})$ combines various slowly varying factors, which are not relevant for the subsequent discussion. (One may note that the function $m_{\mathbf{p}}$ is dependent of the gauge

adopted for the description of the laser field and that it is a constant for a zero-range potential). The decisive factor is the exponential of the action

$$S_{\mathbf{p}}(t,t',\mathbf{k}) = -\frac{1}{2}\int_t^\infty d\tau[\mathbf{p}+\mathbf{A}(\tau)]^2 - \frac{1}{2}\int_{t'}^t d\tau[\mathbf{k}+\mathbf{A}(\tau)]^2 + \int_{-\infty}^{t'} d\tau I_p, \tag{6}$$

which combines terms of the Volkov functions and the initial state. The action is written in a suggestive form that recalls the simple-man rescattering picture: the field-free initial state with ionization potential I_p for times between $-\infty$ and t', propagation in the Coulomb-free continuum in between the ionization time t' and the recollision time t, and Coulomb-free propagation towards the detector with the final drift momentum $\mathbf{p}$ thereafter.

There are essentially two possibilities to evaluate the amplitude. One method is limited to monochromatic sinusoidal plane-wave fields. One may then expand the action $S(t,t',\mathbf{k})$ in a product of series of Bessel functions. One of the two temporal integrals can be carried out analytically and yields the δ function

$$\delta(\mathbf{p}^2/2 - I_p - U_p - n\omega), \tag{7}$$

which expresses energy conservation with the absorption of n photons with energy $\hbar\omega$ from the laser field. Here, $U_p = \langle\mathbf{A}^2(t)\rangle_t/2 = I/(4\omega^2)$ denotes the ponderomotive energy ($\langle\dots\rangle_t$ is the average over one period of the field and I its intensity; for a linearly polarized field with the vector potential $\mathbf{A}(t) = \hat{\mathbf{x}}A_0\cos(\omega t+\phi)$ we have $U_p = A_0^2/4$). Actually, since the description relies on a classical external field, there are no photons. The term $n\omega$ with $\omega = 2\pi/T$ and T the period of the field reflects the temporal periodicity of the field environment. The remaining temporal integral and the sums have to be carried out numerically.

The alternative is an evaluation of the integrals over t and t' by the method of steepest descent (stationary phase). To this end, we determine the stationary points of the action (6), which are given by the solutions $(t,t',\mathbf{k})_s$ of $\partial S/\partial t = \partial S/\partial t' = 0$ and $\partial S/\partial\mathbf{k} = \mathbf{0}$, i.e. by the solutions of the so-called saddle-point equations [12]

$$\left[\mathbf{k}+\mathbf{A}(t')\right]^2 = -2I_p, \tag{8a}$$

$$(t-t')\mathbf{k} = -\int_{t'}^t d\tau\mathbf{A}(\tau), \tag{8b}$$

$$[\mathbf{k}+\mathbf{A}(t)]^2 = [\mathbf{p}+\mathbf{A}(t)]^2, \tag{8c}$$

which physically describe energy conservation at the time t' of ionization, return of the electron to its parent ion at the time t, and elastic scattering at this time into the final state with drift momentum $\mathbf{p}$. The only numerical work consists in the solution of the saddle-point equations (8). However, this may be not completely straightforward, especially if the laser field has significant ellipticity. For fixed asymptotic momentum $\mathbf{p}$, Eqs. (8) have more than one solution, and we number them by the index s. Given these solutions $(t,t',\mathbf{k})_s$ ($s = 1,2,\dots$), the saddle-point approximation to the amplitude is

$$M_{\mathbf{p}}^{(1)} = \sum_s \left(\frac{(2\pi i)^5}{\det(\partial^2 S/\partial q_j^{(s)}\partial q_k^{(s)})_{j,k=1,\dots,5}}\right)^{1/2} e^{iS(t_s,t_s',\mathbf{k}_s)}, \tag{9}$$

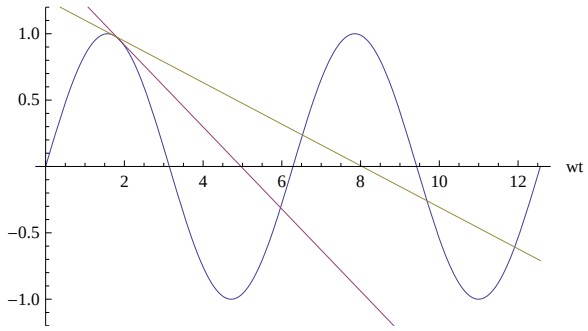

FIG. 1: (Color online) Graphical determination of the rescattering time t from the given ionization time t'. The return condition $x(t) = 0$ can be written in the form $F(t) = F(t') + (t - t')F'(t')$ [10] where $F(t) = \int^t d\tau A(\tau)$ is represented by the (blue) sinusoidal curve. The return condition requires to put the tangent to the curve $F(t)$ at the ionization time t'. The subsequent intersection $(t > t')$ of the tangent with the curve $F(t)$ determines the rescattering time. Two examples are given: The ionization time $\omega t' = 108°$ determines the rescattering time for the situation where the return energy assumes its maximum of $3.17\,U_p$ (pink tangent). There is only one solution for the rescattering time in this case. The ionization time $\omega t' = 99°$ determines three solutions for the rescattering time (yellow tangent), and ionization times closer and closer to 90° lead to more and more such solutions.

where $q_i^{(s)}$ $(i = 1, \ldots, 5)$ combines the five variables t_s, t'_s, and $\mathbf{k}_s$. Actually, the sum over s runs only over a subset of all solutions of the saddle-point equations, namely those through which the original multidimensional integration contour must be routed. We notice that owing to Eq. (8a) the solutions $(t, t', \mathbf{k})_s$ $(s = 1, 2, \ldots)$ must be complex. It is interesting to note that the quantum-orbit representation of the rescattering amplitude is a realization of the quantum-mechanical path integral [10].

The purpose of the present paper is to review recently obtained additional support for the physical relevance of the concept of quantum orbits, especially for the significance of the so-called "longer orbits." As already mentioned, for fixed drift momentum $\mathbf{p}$, the saddle-point equations may have more than one relevant solution for t, t', and $\mathbf{k}$. This can easily be seen (cf. Fig. 1). Their contributions must be included, in general, to obtain a quantitatively good approximation to the amplitude (2). However, in two cases their contributions are even qualitatively crucial: for elliptical polarization and for the description of the so-called intensity-dependent enhancements within the rescattering plateau. In the first case, the dominant contribution to the ionization amplitude is not provided by the two shortest orbits (as is normally the case) but originates from longer orbits. In the second case, the enhancements only come about by the coherent superposition of the contributions of very many long orbits. We shall discuss recent measurements for elliptical polarization that confirm this point [7], and new results regarding the existence of the afore-mentioned enhancements in molecules [8] where it had been in question. The origin of the longer orbits is explained in Fig. 1; an illustration of the shortest and some longer quantum orbits for elliptical polarization is given in Fig. 2.

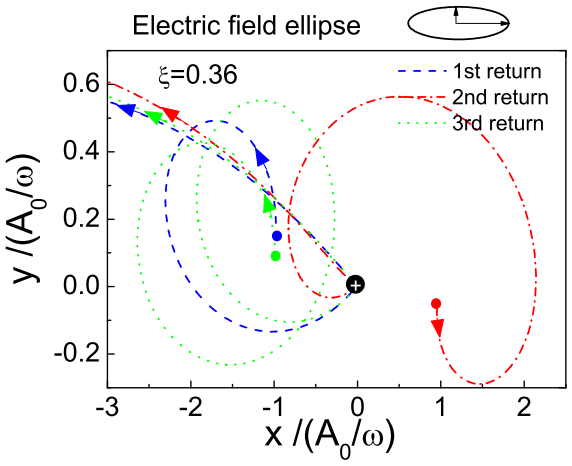

FIG. 2: (Color online) Real parts of quantum orbits in an elliptically polarized laser field with ellipticity $\xi = 0.36$. The field ellipse is depicted in the upper right corner of the figure. The position of the ion is marked by the black dot at the origin. The orbits start at the respective "tunnel exits," which are given by $\mathrm{Re}\,(\mathbf{x}(\mathrm{Re}t'_s))$, and are located away from the position of the ion, mostly in the direction of the major axis of the elliptically polarized field. Depending on the direction of the field at the time t' of ionization, the tunnel exit can be on either side of the ion. Some typical orbits are presented, which become more and more complicated as the travel time increases. All orbits shown have the same drift momentum, which is the momentum at the detector outside the field. Note the different scale of the two axes.

III. LONGER ORBITS FOR AN ELLIPTICALLY POLARIZED LASER FIELD

Within the simple-man model [13], the electron is usually assumed to start its orbit at the "exit of the tunnel" with zero velocity. However, for elliptical polarization, if it starts with zero velocity it will not, in general, revisit the ion: if it does revisit in the direction of the major axis at the time t, it will be off in the direction of the minor axis. Formally, this can be seen from the saddle-point equations (8). Consider the limit $I_p = 0$, which corresponds to the simple-man model, and a specified final momentum $\mathbf{p}$. For linear polarization in the x direction, Eq. (8b) requires that $k_y = k_z = 0$. The remaining three equations (8) are then solved in terms of the three variables t, t', and k_x, and the initial velocity is $v_x(t') \equiv k_x + A_x(t') = 0$. For elliptical polarization in the (x, y) plane, we have $k_z = 0$, and the remaining four equations are solved in terms of the four variables t, t', k_x, and k_y. However, it is no longer possible that the initial velocity be zero since we cannot have, in general, that both $v_x(t') = k_x + A_x(t') = 0$ and $v_y(t') = k_y + A_y(t') = 0$.

However, while such a nonzero initial velocity does allow the electron to revisit its parent ion, the weight of such an orbit will be substantially reduced. Therefore, rescattering processes continue to occur for elliptical polarization but at reduced yields. Another consequence is: for linear polarization, normally the shortest orbits dominate the ionization

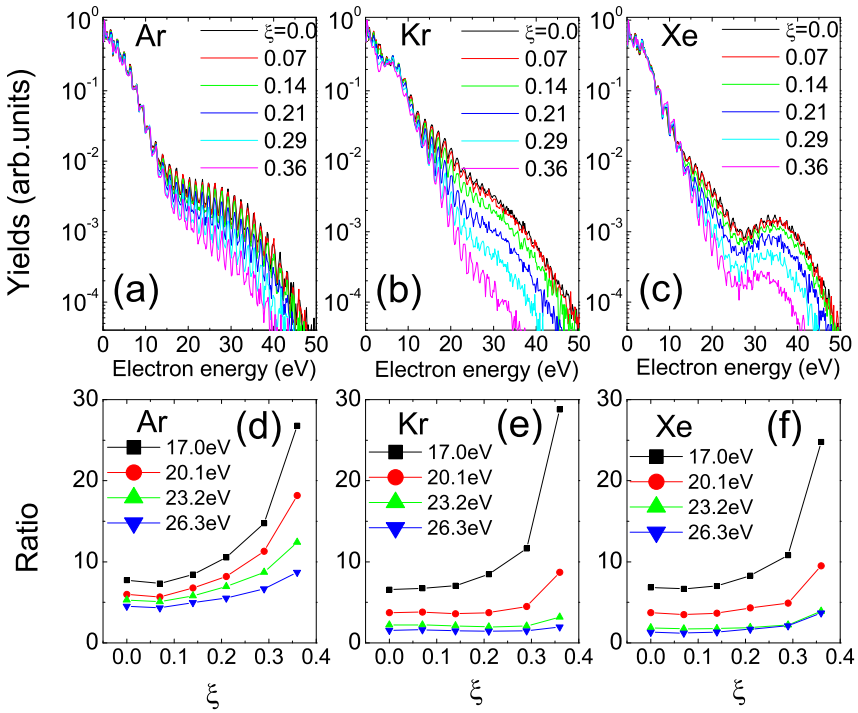

FIG. 3: (Color online) Experimental [(a), (b), and (c)] photoelectron spectra of Ar, Kr, and Xe along the major polarization axis for elliptically polarized laser pulses with wavelength of 800 nm, intensity of 7.0×10^{13}W/cm^2, and ellipticities $\xi = 0$, 0.07, 0.14, 0.21, 0.29, and 0.36 from top to bottom. The spectra are normalized to unity at zero energy. (d)–(f): Ratios of the electron yields for various low-energy intervals over one high-energy interval as functions of the ellipticity. For details, see the text.

amplitude. The contributions of the longer orbits are increasingly suppressed by quantum-mechanical wave function spreading. They cause some modifications of the spectrum but do not qualitatively change it. (An exception is provided by the intensity-dependent enhancements, which will be considered in the next Section.) This is different as soon as the polarization is sufficiently elliptical. Then, those orbits have the highest yield that require the smallest magnitude of the initial velocity in order to revisit. Those are not necessarily the shortest orbits [14] because the longer the travel time is the smaller is the transverse initial momentum that is required in order that the electron revisit the ion [14]. This can also be realized by inspection of the orbits of Fig. 1.

Experimental evidence for substantial contributions of longer orbits in ATI with elliptical polarization was presented in Ref. [10], but no quantitative comparison with quantum-orbit theory was attempted. Here we will report the results of recent measurements and

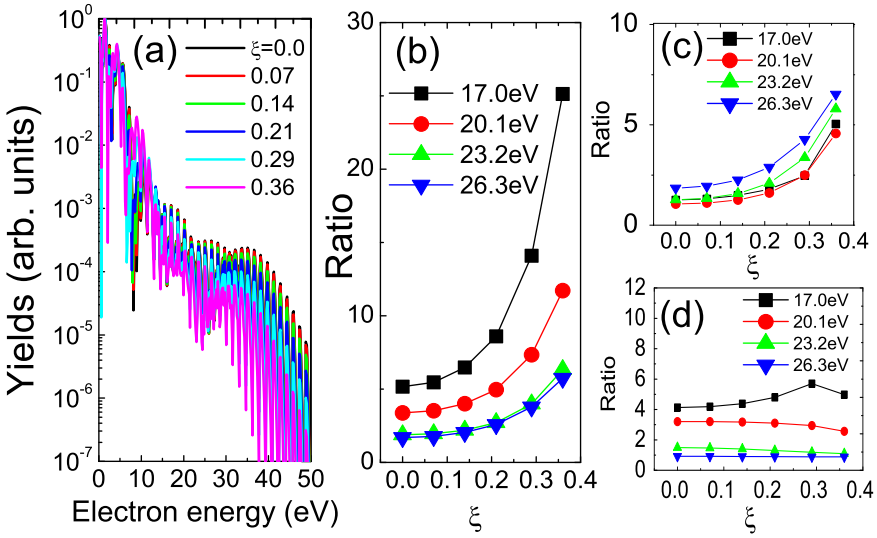

FIG. 4: (Color online) (a) The calculated focal-averaged photoelectron spectra of Ar along the major polarization axis for the ellipticities $\xi = 0$, 0.07, 0.14, 0.21, 0.29, and 0.36 from top to bottom. (b) Similar to Fig. 1(d) but for the theoretical calculation, in which the first twenty pairs of quantum orbits are included. (c) Similar to (b), but only the first pair of orbits is considered in the calculation. (d) Ratio of the two ratios in (b) and (c). The laser parameters are chosen as the wavelength of 800 nm and the intensity of 6.2×10^{13} W/cm^2, slightly lower than the one estimated for the experiment. Such procedure has been standard practice in SFA calculations; see, e.g., Ref. [15].

compare them with theory [7].

Figure 3 exhibits experimental ATI spectra along the major polarization axis for the three rare gases Ar, Kr, and Xe for ellipticities up to $\xi = 0.36$. After normalization in order to compensate the general decrease with increasing ellipticity the spectrum of the direct electrons is all but independent of ellipticity, and the onset of rescattering is very clearly visible. Our goal is quantitatively to support the quantum-orbit picture. To this end, we plot the ratios of the electron yields in four adjacent energy windows in the beginning and the middle of the plateau over the yield in a high-energy window as a function of ellipticity. Each window is defined so as to contain two ATI peaks. The windows extend from 17.0 to 20.1 eV, from 20.1 to 23.2 eV, from 23.2 eV to 26.3 eV, and from 26.3 to 29.4 eV, and the ratio is formed with the yield in the window from 37.0 to 40.1 eV. Since the rescattering plateau is more like an inclined plane, all of the ratios are larger than unity. Since the inclination of the plateau becomes stronger when the ellipticity is higher, the ratios increase strongly with increasing ellipticity.

In Fig. 4 we compare the experimental data with the quantum-orbit theory reviewed in the preceding Section. For simplicity, we took a zero-range potential to bind the electron to the ion in place of a Coulomb-like potential. This renders the description of the direct electrons unreliable; so the reader should ignore the discrepancy between the spectra in

Figs. 3(a) and 4(a) for energies below about 10 eV. We will focus on the rescattered electrons and calculate, for argon, the same ratios as in Fig. 3. The results are plotted in panel (b), which should be compared with Fig. 3(d). The agreement is quite good. The calculation was based on including the first 20 pairs of quantum orbits. Now, in order to assess the significance of the contributions of the longer orbits, we repeat the calculation including only the first pair of orbits. The result is shown in Fig. 4(c). Clearly, the good agreement is gone, definitely for the low-energy ratio. This proves a substantial contribution of the longer orbits especially to the low-energy part of the rescattering plateau. Finally, in Fig. 4(d) we plot the ratio of the two ratios in (b) and (c), which roughly gives the number of the contributing pairs of orbits. It goes up from unity for small ellipticity and high energy to 5 or 6 at large ellipticity and low energy. This confirms that the long orbits are especially important for the low-energy part of the plateau [14]. Similar conclusions were drawn from SFA simulations of nonsequential double ionization [16] as well as from completely classical trajectory calculations [17].

IV. INTENSITY-DEPENDENT ENHANCEMENTS OF GROUPS OF PEAKS IN THE RESCATTERING PLATEAU

The rescattering plateau has an essentially classical origin: backscattering allows the electron an additional acceleration by a full half cycle of the laser field, which leads to a maximal classical energy of $10\,U_p$. However, the plateau also exhibits a fascinating feature, which appears to be of quantum origin: in some cases, if the laser intensity is raised by as little as a few percent, the yield of a group of peaks within the plateau may rear up by almost an order of magnitude [18, 19]. Typically, this may happen in the middle part of the plateau, for energies between 6 and 8 times the ponderomotive energy U_p. The physical origin of this phenomenon is still controversial. Essentially, two different mechanisms have been proposed.

The effect is reminiscent of an intensity-dependent resonance. Indeed, it was suggested that it is due to a multiphoton resonance with an intensity-dependent excited bound state [20–23], much like the well-known Freeman resonances in the low-energy region [24]. A different mechanism – and the one that we will here pursue – is in the context of the strong-field approximation and the quantum-orbit picture. At first sight, it appears that quantum orbits are unable to generate these very sharply defined features, because each individual orbit depends very smoothly on the laser intensity and the electron energy. However, on closer inspection it turns out that the effect comes about by constructive interference of a large number of quantum orbits with the same final energy, which by necessity then have a very long travel time, as we call the time $t - t'$ between rescattering and ionization [11, 15, 25–30]. The conditions for such a constructive interference are satisfied near channel closings (CCs), i.e. if the parameter

$$\eta \equiv (I_p + U_p)/\omega \tag{10}$$

has an integer value n with $n > n_{\min} = [I_\mathrm{p}/\omega]$ and $[x]$ the largest integer contained in x.

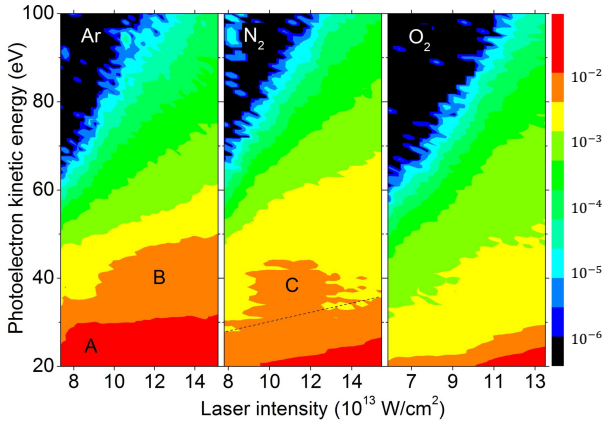

FIG. 5: (Color online). Measured photoelectron energy spectra in the direction along the laser polarization as functions of the laser intensity for the three gas targets Ar, N_2, and O_2, from left to right. The spectra are recorded with 30 fs, 800 nm laser pulses. The laser intensity is displayed in multiples of 10^{13} W/cm^2. Note that $2\,U_\mathrm{p} = 9.56$ eV at 8×10^{13} W/cm^2. Argon displays two well-defined enhancements in the energy region of 25 to 30 eV at about 8×10^{13} W/cm^2 (area A) and between 35 and 45 eV at about 9×10^{13} W/cm^2 (area B), N_2 exhibits an analog of the enhanced area B in area C, while for O_2 no enhancements are visible. The $10\,U_p$ cutoff of the backscattering plateau is clearly visible.

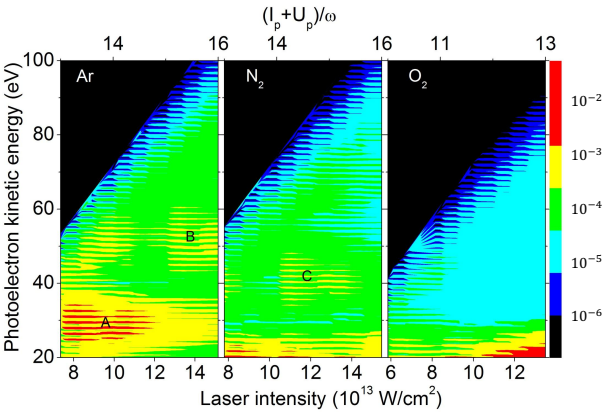

FIG. 6: (Color online). Calculated spectra for Ar, N_2, and O_2. The laser intensity is also displayed in terms of the parameter $\eta = (I_\mathrm{p} + U_\mathrm{p})/\omega$ [Eq. (10)] to demonstrate the channel-closing effect. Parameters in the simulation are chosen in accordance with the experiments. The areas labeled A, B, and C approximately correspond to those in Fig. 5.

When the laser intensity varies such that a CC is passed, the minimum number of photons required for ionization changes by one. (We refer to the intensity, for which $\eta = n$, by I_n.) Just above a CC, intermediate states with very low momenta allow the electron many times to revisit its parent ion. The sensitive dependence on the laser intensity, which is absent from each individual quantum orbit, comes about by the interference of a large number of them, each corresponding to rescattering at one of these revisits. A closely related explanation invokes the so-called threshold anomalies in the detachment of electrons bound by short-range potentials [31, 32], see also Ref. [11].

Both explanations are capable of reproducing the data quite well. This appears surprising since the first mechanism crucially depends on the existence of excited bound states, which are completely absent from the latter. On the other hand, the assumption of an "effective continuum threshold" in the context of the SFA may provide a description that captures essential aspects of Rydberg states [26].

Multiphoton ionization of molecules has come a long way since the first attempts to confirm the I^N behavior of the total ionization rates [33]. Here we will present measurements of ATI spectra in N_2 and O_2 (and compare them with Ar) that exhibit noticeable enhancements in N_2 but not in O_2 and describe them in terms of the molecular SFA [34] and ISFA [35]. The presence or absence of these enhancements in molecules still is an open issue. Cornaggia [36] observed enhancements in H_2 but not in more complicated molecules.

The spectra were recorded with 30-fs laser pulses with a center wavelength of 800 nm. Details of the experimental setup can be found in Ref. [37, 38]. Figure 5 displays photoelectron energy spectra in the laser polarization direction for Ar, N_2, and O_2 at various intensities as given in the caption. For each intensity, the spectrum was separately normalized in order to compensate the general increase of the yield with increasing intensity. We notice two kinds of structures in Fig. 5: first, there are intensity-dependent structures such as the $10\,U_p$ cutoff, which marks the end of the plateau. Second, there are horizontal structures, which set in at certain well-defined intensities. They are marked by the letters A, B, and C. These we associate with the intensity-dependent enhancements [15, 18, 19] of groups of peaks within the backscattering plateau. They rise rather suddenly at a certain intensity and die out rather slowly when the intensity further increases. The group of peaks concerned remains the same throughout this process. Quantum-orbit theory predicts that the enhancements start at the CC intensities I_n [defined above below Eq. (10)]. For argon, the relevant CC intensities are $I_{13} = 7.34 \times 10^{13}$ W/cm^2 and $I_{14} = 9.94 \times 10^{13}$ W/cm^2, for N_2 they are $I_{13} = 7.64 \times 10^{13}$ W/cm^2 and $I_{14} = 10.2 \times 10^{13}$ W/cm^2. Corresponding spectra at selected fixed intensities can be found in Ref. [8]. The areas B for argon and C for N_2 qualitatively correspond to each other, which confirms the existence of the intensity-dependent enhancements in N_2. However, any such structures are distinctly absent in O_2. These two observations are the most important message of Fig. 5.

Can we understand the absence of the enhancements in O_2? Indeed, if resonance with ponderomotively upshifted Rydberg states were responsible for the enhancements the different behavior of N_2 and O_2 would be hard to understand, in view of the close similarity of the respective Rydberg states (Freeman-type resonances have been identified in both molecules [39, 40]). To answer the question, we carry out quantum-orbit calculations along

the lines of Ref. [35]. Molecular SFA simulations depend on the gauge employed for the description of the laser field. We use the so-called dressed length gauge, which quite well reproduces the suppression of the low-energy yield in O_2 compared with N_2 [41].

Since we are concerned with electron energies above the direct-electron cutoff of $2U_p$, we need to evaluate the rescattering amplitude (2). Molecular information enters this expression via the rescattering potential V and via the ground-state wave function $|\psi_0(t')\rangle$. The potential is modeled by the superposition of target-specific atomic scattering potentials and the wave function has the form of a linear combination of atomic orbitals (LCAO) [30]

$$\sum_a c_a \left[\psi_a^{(0)}(\mathbf{r}+\mathbf{R}_0/2) + (-1)^{l_a-m_a+m_\lambda}\psi_a^{(0)}(\mathbf{r}-\mathbf{R}_0/2)\right]. \tag{11}$$

Here $\mathbf{R}_0$ denotes the relative nuclear coordinate and l_a and m_a the orbital and magnetic quantum numbers while the functions $\psi_a^{(0)}(\mathbf{r})$ are Slater-type orbitals and m_λ is the projection of the orbital angular momentum on the internuclear axis. Compared with rescattering off a single atom, the two-center situation will generate the additional factor

$$M_{\mathbf{p}}^{(1)} \propto \begin{cases} \cos(\mathbf{k}\cdot\mathbf{R}_0/2)\cos((\mathbf{p}-\mathbf{k})\cdot\mathbf{R}_0/2) \text{ for even } l_a, \\ \sin(\mathbf{k}\cdot\mathbf{R}_0/2)\cos((\mathbf{p}-\mathbf{k})\cdot\mathbf{R}_0/2) \text{ for odd } l_a. \end{cases} \tag{12}$$

For the longer orbits, the intermediate momentum $\mathbf{k}$ is small (cf. Fig. 1). Hence, this factor crucially depends on the orbital angular momentum l_a. For N_2, the initial highest occupied molecular orbit (HOMO) is $3\sigma_g$, which is a linear combination of s and p states with almost equal weights. In contrast, for O_2 its initial HOMO is made up only of p states. Therefore, for O_2 the contribution of the long orbits will be much reduced in comparison with N_2.

We find this confirmed by the calculational results, which are presented in Fig. 6. Indeed, for O_2 we find the entire plateau much weaker than for N_2 and there is hardly any trace of enhancements. The agreement with the experimental data of Fig. 5 is quite satisfactory. The fact that the experimentally observed existence of the intensity-dependent enhancements in N_2 and their absence in O_2 can be reproduced by quantum-orbit theory lends further support to the physical significance of quantum orbits and, especially, to that of the longer orbits.

V. CONCLUSIONS

Quantum orbits are a physically appealing and also a very powerful tool, which is able to describe a multitude of laser-atom phenomena. An unvoidable consequence of the derivation of the expansion into quantum orbits from the strong-field approximation is the fact that there are many quantum orbits contributing to a given amplitude, which take a longer and longer time between ionization and rescattering. However, the physical significance of these long orbits appears questionable, since they disregard the Coulomb potential except in the very process of rescattering. Whenever a classical recolliding electron passes its parent ion at a short distance, it will be attracted by the Coulomb field and

significantly deflected from its original course. Especially the motion transverse to the laser polarization, whose momentum is conserved in the ISFA except in the recollision, is strongly affected and will have little in common with the trajectory without the Coulomb field. This seems to imply that the longer orbits – where the crucial interaction with the Coulomb potential occurs at the occasion of not the first but a subsequent revisit – are void of physical significance.

However, this is not necessarily the case in the quantum description. In this paper, we presented additional support for the quantum-orbit description. First, whenever long and very long orbits play a substantial role, then quantum-orbit theory trivially predicts that the effect in question, such as the intensity-dependent enhancements discussed above, will go away for short pulses. Indeed, this has been observed for the ATI enhancements [42]. Second, we investigated these enhancements for the case of molecules, found them to exist for N_2 but not for O_2, and successfully described the experimental data in terms of quantum-orbit theory. We emphasize again that the intensity-dependent enhancements appear to be a quantum effect, which is inaccessible to classical modeling. We also considered above-threshold ionization by an elliptically polarized laser field. In this case, quantum-orbit theory predicts that the spectrum is qualitatively dominated by substantial contributions of longer orbits. We found this confirmed and obtained good agreement when we compared our experimental spectra with the quantum-orbit simulations.

The exact reason of why the quantum-orbit description of the effects here described works so well remains unclear. This is puzzling because the description crucially depends on the longer orbits, which appear to have so little in common with classical Coulomb-affected trajectories. On the other hand, the ISFA can be evaluated without recourse to the quantum-orbit expansion as briefly discussed above around Eq. (7). In this context, near channel closings the integration over the travel time has to be extended over very many periods of the field while away from CCs at most two periods normally suffice. Quantum orbits are a very convenient tool for the calculation as well as for the interpretation, but their use is not mandatory. In the frame of the finite-range quasi-energy method, the enhancements occur as well and are subsumed under the term "threshold anomalies" [31, 32]. Finally, we mention that all of the Coulomb-related complications are absent for the otherwise closely related case of multiphoton detachment of negative ions. In this case, the quantum-orbit expansion is a quantitatively reliable tool, see e.g. Ref. [43].

VI. ACKNOWLEDGMENTS

This work was supported by the National Basic Research Program of China (Nos. 2013CB922201 and 2011CB808102) and NNSF of China (Nos. 10925420, 10904162, and 11174330, and 11274050). Sponsorship has also been provided by the Alexander von Humboldt Foundation and funding by the German Federal Ministry of Education and Research in the framework of the Research Group Linkage Program.

References

[1] L. V. Keldysh, Zh. Eksp. Teor. Fiz. **47**, 1945 (1964) [Sov. Phys.-JETP **20**, 1307]; F. H. M. Faisal, J. Phys. B **6**, L89 (1973).
[2] H. R. Reiss, Phys. Rev. A **22**, 1786 (1980)
[3] M. Lewenstein, Ph. Balcou, M. Yu. Ivanov, A. L'Huillier, and P. B. Corkum, Phys. Rev. A **49**, 2117 (1994).
[4] W. Becker, A. Lohr, and M. Kleber, J. Phys. B **27**, L325 (1994) [Corrigendum: J. Phys. B **28**, 1931 (1995)].
[5] F. Krausz and M. Ivanov, Rev. Mod. Phys. **81**, 163 (2009).
[6] D. B. Milošević, D. Bauer, and W. Becker, J. Mod. Opt. **53**, 125 (2006).
[7] XY. Lai, CL. Wang, YJ. Chen, ZL. Hu, W. Quan, XJ. Liu, J. Chen, Y. Chang, ZZ. Xu, and W. Becker, Phys. Rev. Lett. **110**, 043002 (2013).
[8] W. Quan, XY. Lai, YJ. Chen, CL. Wang, ZL. Hu, XJ. Liu, XL. Hao, J. Chen, E. Hasović, M. Busuladžić, W. Becker, and D. B. Milošević, Phys. Rev. A **88**, 021401(R) (2013).
[9] R. Kopold, W. Becker, and M. Kleber, Opt. Commun. **179**, 39 (2000).
[10] P. Salières, B. Carré, L. le Déroff, F. Grasbon, G. G. Paulus, H. Walther, R. Kopold, W. Becker, D. B. Milošević, A. Sanpera, and M. Lewenstein, Science **292**, 902 (2001).
[11] D. B. Milošević, E. Hasović, M. Busuladžić, A. Gazibegović-Busuladžić, and W. Becker, Phys. Rev. A **76**, 053410 (2007).
[12] We treat the term $\exp[i\mathbf{A}(t)\cdot\mathbf{r}]$ as slowly varying.
[13] H. B. van Linden van den Heuvell and H. G. Muller, in "Multiphoton Processes" (edited by S. J. Smith and P. L. Knight), Vol. 8 of Cambridge Studies of Modern Optics (Cambridge University Press, Cambridge), p. 25 (1988).
[14] R. Kopold, D. B. Milošević, and W. Becker, Phys. Rev. Lett. **84**, 3831 (2000).
[15] D. B. Milošević, W. Becker, M. Okunishi, G. Prümper, K. Shimada, and K. Ueda, J. Phys. B **43**, 015401 (2010).
[16] N. I. Shvetsov-Shilovski, S. P. Goreslavski, S. V. Popruzhenko, and W. Becker, Phys. Rev. A **77**, 063405 (2008).
[17] X. Wang and J. H. Eberly, New J. Phys. **12**, 093047 (2010).
[18] M. P. Hertlein, P. H. Bucksbaum, and H. G. Muller, J. Phys. B **30**, L197 (1997).
[19] P. Hansch, M. A. Walker, and L. D. Van Woerkom, Phys. Rev. A **55**, R2535 (1997).
[20] H. G. Muller and F. C. Kooiman, Phys. Rev. Lett. **81**, 1207 (1998); H. G. Muller, Phys. Rev. Lett. **83**, 3158 (1999); Phys. Rev. A **60**, 1341 (1999).
[21] E. Cormier, D. Garzella, P. Breger, P. Agostini, G. Chériaux, and C. Leblanc, J. Phys. B **34**, L9 (2001).
[22] J. Wassaf, V. Véniard, R. Taïeb, and A. Maquet, Phys. Rev. Lett. **90**, 013003 (2003).
[23] R. M. Potvliege and S. Vučić, Phys. Rev. A **74**, 023412 (2006); J. Phys. B **42**, 055603 (2009).
[24] R. R. Freeman, P. H. Bucksbaum, H. Milchberg, S. Darack, D. Schumacher, and M. E. Geusic, Phys. Rev. Lett. **59**, 1092 (1987).
[25] R. Kopold and W. Becker, J. Phys. B **32**, L419 (1999).
[26] G. G. Paulus, F. Grasbon, H. Walther, R. Kopold, and W. Becker, Phys. Rev. A **64**, 021401(R) (2001).
[27] R. Kopold, W. Becker, M. Kleber, and G. G. Paulus, J. Phys. B **35**, 217 (2002).
[28] S. V. Popruzhenko, Ph. A. Korneev, S. P. Goreslavski, and W. Becker, Phys. Rev. Lett. **89**, 023001 (2002).
[29] E. Hasović, M. Busuladžić, A. Gazibegović-Busuladžić, D. B. Milošević, and W. Becker, Laser Phys. **17**, 376 (2007).

[30] D. B. Milošević, E. Hasović, S. Odžak, M. Busuladžić, A. Gazibegović-Busuladžić, and W. Becker, J. Mod. Opt. **55**, 2653 (2008).
[31] B. Borca, M. V. Frolov, N. L. Manakov, and A. F. Starace, Phys. Rev. Lett. **88**, 193001 (2002).
[32] M. V. Frolov, N. L. Manakov, and A. F. Starace, Phys. Rev. A **79**, 033406 (2010).
[33] S. L. Chin, Phys. Rev. A **4**, 992 (1971).
[34] D. B. Milošević, Phys. Rev. A **74**, 063404 (2006).
[35] M. Busuladžić, A. Gazibegović-Busuladžić, D. B. Milošević, and W. Becker, Phys. Rev. Lett. **100**, 203003 (2008); Phys. Rev. A **78**, 033412 (2008).
[36] C. Cornaggia, Phys. Rev. A **82**, 053410 (2010).
[37] W. Quan, Z. Lin, M. Wu, H. Kang, H. Liu, X. Liu, J. Chen, J. Liu, X. T. He, S. G. Chen, H. Xiong, L. Guo, H. Xu, Y. Fu, Y. Cheng, and Z. Z. Xu, Phys. Rev. Lett. **103**, 093001 (2009).
[38] H. Kang, W. Quan, Y. Wang, Z. Lin, M. Wu, H. Liu, X. Liu, B. B. Wang, H. J. Liu, Y. Q. Gu, X. Y. Jia, J. Liu, J. Chen, and Y. Cheng, Phys. Rev. Lett. **104**, 203001 (2010).
[39] T. Kłoda, A. Matsuda, H. O. Karlsson, M. Elshakre, P. Linusson, J. H. D. Eland, R. Feifel, and T. Hansson, Phys. Rev. A **82**, 033431 (2010).
[40] G. N. Gibson, R. R. Freeman, and T. J. McIlrath, Phys. Rev. Lett. **67**, 1230 (1991).
[41] M. Busuladžić and D. B. Milošević, Phys. Rev. A **82**, 015401 (2010).
[42] F. Grasbon, G. G. Paulus, H. Walther, P. Villoresi, G. Sansone, S. Stagira, M. Nisoli, and S. De Silvestri, Phys. Rev. Lett. **91**, 173003 (2003).
[43] A. Gazibegović-Busuladžić, D. B. Milošević, W. Becker, B. Bergues, H. Hultgren, and I. Yu. Kiyan, Phys. Rev. Lett. **101**, 103004 (2010).